CMS Physics Analysis Summary

Contact: cms-pag-conveners-susy@cern.ch 2011/04/05

Further interpretation of the search for supersymmetry based on α_T

The CMS Collaboration

Abstract

A first search for supersymmetry in events with jets and missing energy was carried out in Phys. Lett. B 698 (2011) 196, using 35 pb^{-1} of integrated luminosity at $\sqrt{s}$ = 7 TeV. In this search, the variable α_{T} was used as the main discriminator between events with real and fake missing transverse energy and no excess of events over the Standard Model expectation was found. In this note an extended interpretation of the above result is presented. The dependence of the exclusion limit on the tan β parameter of the Constrained Minimal Supersymmetric extension of the Standard Model is studied. Furthermore, upper limits on the cross section for different Simplified Model Spectra are presented.

1 Introduction

In this note additional material and an extended interpretation of the results of Ref. [1] are presented. These additional interpretations are based on the full selection, definition of signal and background control regions, as well as the data driven background methods of the above search. No re-analysis of the data or changes in the cutflow are carried out.

For the Constrained Minimal Supersymmetric extension of the Standard Model (CMSSM) [2] 95% CL exclusion limits are derived in the $(m_0, m_{1/2})$ plane for three different values of $\tan\beta$ (3, 10 and 50) and the 68% CL ranges around the expected limits have been determined. In addition, efficiency maps of the analysis in the $(m_0, m_{1/2})$ plane are provided.

Furthermore, the analysis results are interpreted for two more generic Simplified Model Spectra (SMS) [3–5] where efficiency maps for the analysis and limits on the production cross section are provided.

2 Summary of analysis and results

In the following we give a brief summary of the analysis in Ref. [1], which selects events with two or more high-p_{T} jets. Specifically, jets are reconstructed using the anti-k_{T} algorithm [6] with a size parameter of 0.5 and are required to have $E_{\mathrm{T}} > 50\,\mathrm{GeV}$, $|\eta| < 3$ and to pass jet identification criteria [7] designed to reject spurious signals in the calorimeters. The pseudorapidity of the jet with the highest E_{T} (leading jet) is required to be within $|\eta| < 2.5$ and the transverse energy of each of the two leading jets must exceed 100 GeV.

Events with jets passing the E_{T} threshold but not satisfying the jet identification criteria or the η acceptance requirement are vetoed, as this deposited energy is not accounted for in the event kinematics. Similarly, events in which an isolated lepton (electron [8] or muon [9]) with $p_{\mathrm{T}} > 10\,\mathrm{GeV}$ is identified are rejected to suppress events with genuine missing energy from neutrinos. Furthermore, to select a pure multi-jet topology, events are vetoed in which an isolated photon [10] with $p_{\mathrm{T}} > 25\,\mathrm{GeV}$ is found.

Events are required to fulfill $H_{\mathrm{T}} = \sum_{i=1}^{\mathrm{N_{jet}}} {E_{\mathrm{T}}}^{\mathrm{j}_i} > 350\,\mathrm{GeV}$. As the main discriminator against QCD multijet production the variable α_{T}, defined as:

$$\alpha_{\mathrm{T}} = \frac{{E_{\mathrm{T}}}^{\mathrm{j}_2}}{M_{\mathrm{T}}} = \frac{{E_{\mathrm{T}}}^{\mathrm{j}_2}}{\sqrt{\left(\sum_{i=1}^{2} {E_{\mathrm{T}}}^{\mathrm{j}_i}\right)^2 - \left(\sum_{i=1}^{2} p_x^{\mathrm{j}_i}\right)^2 - \left(\sum_{i=1}^{2} p_y^{\mathrm{j}_i}\right)^2}}, \tag{1}$$

is used for the two jet case and events are required to have $\alpha_{\mathrm{T}} > 0.55$. For larger jet multiplicities, the n-jet system is reduced to a di-jet system by combining the jets in the event into two pseudo-jets. The E_{T} of each of the two pseudo-jets is calculated as the scalar sum of the contributing jet E_{T}'s. The combination chosen is the one that minimizes the E_{T} difference between the two pseudo-jets. The such defined pseudo-jets are then used in Equation 1 to calculate α_{T}.

To protect against severe energy losses, events with significant jet mismeasurements caused by masked regions in the ECAL, which amount to about 1% of the ECAL channel count, are removed with the following procedure. The jet-based estimate of the missing transverse energy, $\not{H}_{\mathrm{T}} = |\vec{\not{H}}_{\mathrm{T}}| = |-\sum_{\mathrm{jets}} \vec{p}_{\mathrm{T_{jet}}}|$, is used to identify the jet most likely to have given rise to the $\not{H}_{\mathrm{T}}$ as the jet whose momentum is closest in ϕ to the total $\vec{\not{H}}_{\mathrm{T}}$ which results after removing the jet from the event. The azimuthal distance between this jet and the recomputed $\not{H}_{\mathrm{T}}$ is referred to

as $\Delta\phi^*$ in what follows. Events with $\Delta\phi^* < 0.5$ are rejected if the distance in the (η, ϕ) plane between the selected jet and the closest masked ECAL region, ΔR_{ECAL}, is smaller than 0.3.

Finally, to protect against multiple jets failing the $E_{\mathrm{T}} > 50\,\mathrm{GeV}$ selection requirement, the jet-based estimate of the missing energy, $\not{H}_{\mathrm{T}}$, is compared to the calorimeter tower-based estimate, $\not{E}_{\mathrm{T}}^{\mathrm{calo}}$, and events with $R_{\mathrm{miss}} = \not{H}_{\mathrm{T}} / \not{E}_{\mathrm{T}}^{\mathrm{calo}} > 1.25$ are rejected.

This selection results in 13 observed events in a data sample of 35 pb^{-1}.

The SM backgrounds were determined with the help of three data driven methods using control regions in H_{T}, and muon+jets and photon+jets control samples.

The total background, consisting of QCD multijet production, $\mathrm{t\bar{t}}$, W+jets and $\mathrm{Z} \to \nu\nu$ + jets events, was estimated by extrapolating the ratio of events passing $\alpha_T > 0.55$ over those failing this requirement, from a low H_{T} control region of $250 < H_{\mathrm{T}} < 350\,\mathrm{GeV}$ to the signal region with $H_{\mathrm{T}} > 350\,\mathrm{GeV}$. This yields prediction of the total SM background of $9.4^{+4.8}_{-4.0\mathrm{stat}} \pm 1.0_{\mathrm{syst}}$.

In addition, an inclusive muon control sample was used to determine the background contribution from W+jets and $\mathrm{t\bar{t}}$ events, yielding a background estimate of $6.1^{+2.8}_{-1.9\mathrm{stat}} \pm 1.8_{\mathrm{syst}}$ events. Furthermore, a photon+jets control sample was used to estimate the background contribution from $Z \to \nu\nu$+jets events, predicting $4.4^{+2.3}_{-1.6\mathrm{stat}} \pm 1.8_{\mathrm{syst}}$ events.

All of the above background estimations are used in the limit calculation.

3 Additional information in the CMSSM

3.1 68% CL range for the expected 95% CL limit in the CMSSM

For the extraction of the 95% CL limit in the CMSSM, the same statistical procedure as described in Ref. [1] has been used. In addition, for a more comprehensive statistical interpretation and as a measure of quality of the 95% CL in CMSSM, we have determined the 68% CL range for the expected limit. This is illustrated in Fig. 1, which shows the 95% CL excluded region in the CMSSM for $\tan\beta = 3$. The 68% CL range is obtained by generating toy experiments for the event yield in the $H_{\mathrm{T}} > 350\,\mathrm{GeV}$ signal region and in each of the control regions ($250 < H_{\mathrm{T}} < 350\,\mathrm{GeV}$, muon and photon control samples). These toys are generated assuming absence of any signal. From these pseudo-measurements, upper limits are calculated (taking signal contamination in the control samples into account) and the 68% central confidence interval is displayed in the figure. The expected limit is taken as the median of the upper limits from the pseudo-measurements.

In addition, 95% CL limits in the $(m_0, m_{1/2})$ plane for values of $\tan\beta = 10$ and 50 are shown in Figures 2 and 3, respectively.

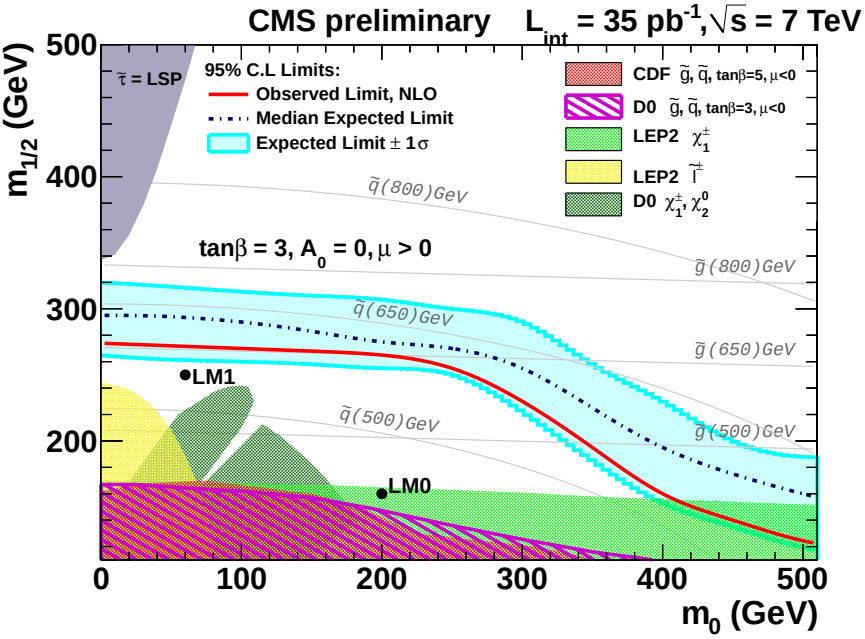

Figure 1: Observed and expected 95% CL exclusion contours in the CMSSM $(m_0, m_{1/2})$ plane ($\tan\beta = 3$, $A_0 = 0$, $\mu > 0$). In addition the 68% CL range for the expected limit is shown.

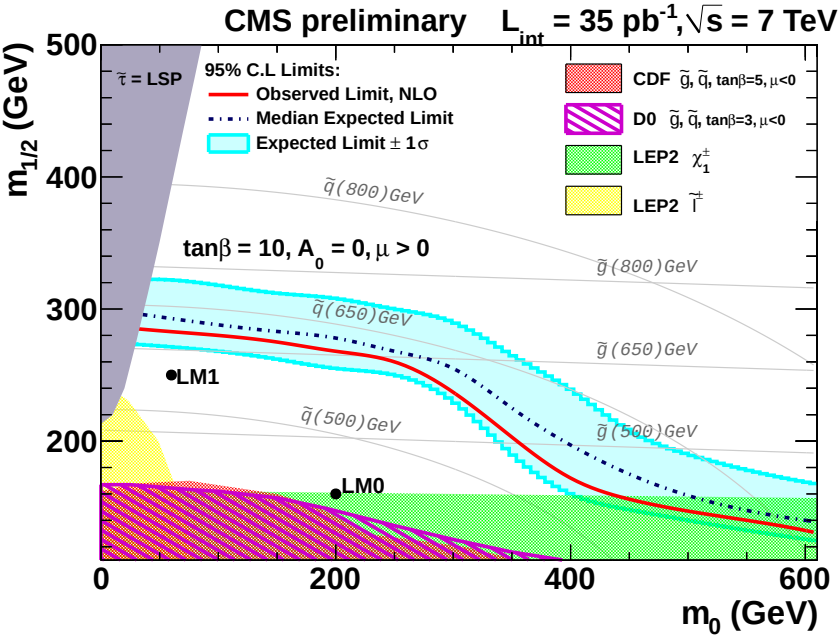

Figure 2: Observed and expected 95% CL exclusion contours in the CMSSM $(m_0, m_{1/2})$ plane ($\tan\beta = 10$, $A_0 = 0$, $\mu > 0$). In addition the 68% CL range for the expected limit is shown.

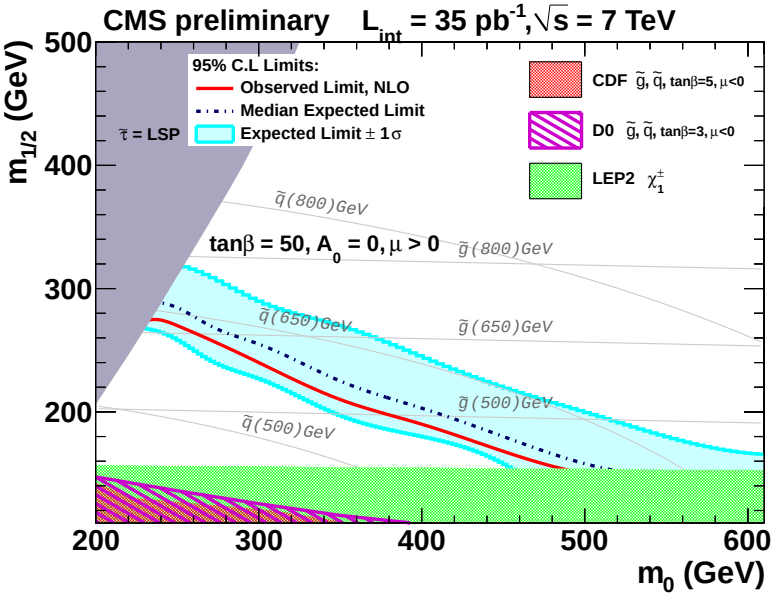

Figure 3: Observed and expected 95% CL exclusion contours in the CMSSM $(m_0, m_{1/2})$ plane ($\tan\beta = 50$, $A_0 = 0$, $\mu > 0$). In addition the 68% CL range for the expected limit is shown.

3.2 Analysis efficiency as a function of m_0 and $m_{1/2}$

Figure 4 shows the variation of the analysis efficiency over the $(m_0, m_{1/2})$ plane in the CMSSM for values of $\tan\beta$ = 3, 10, and 50. The analysis efficiency is defined as the fraction of signal events passing the event selection for any given point in the CMSSM parameter space.

The experimental uncertainties on the efficiency are found to be to good approximation independent of the signal model. They following uncertainties are considered:

- the uncertainty on the luminosity measurement: 11% [1];
- the effect of rejecting events with jets pointing to masked ECAL regions: 3%;
- the modelling of the lepton and photon vetoes: 2.5%;
- the effect of the uncertainty in the jet energy scale and resolution on the selection efficiency: 2.5%.

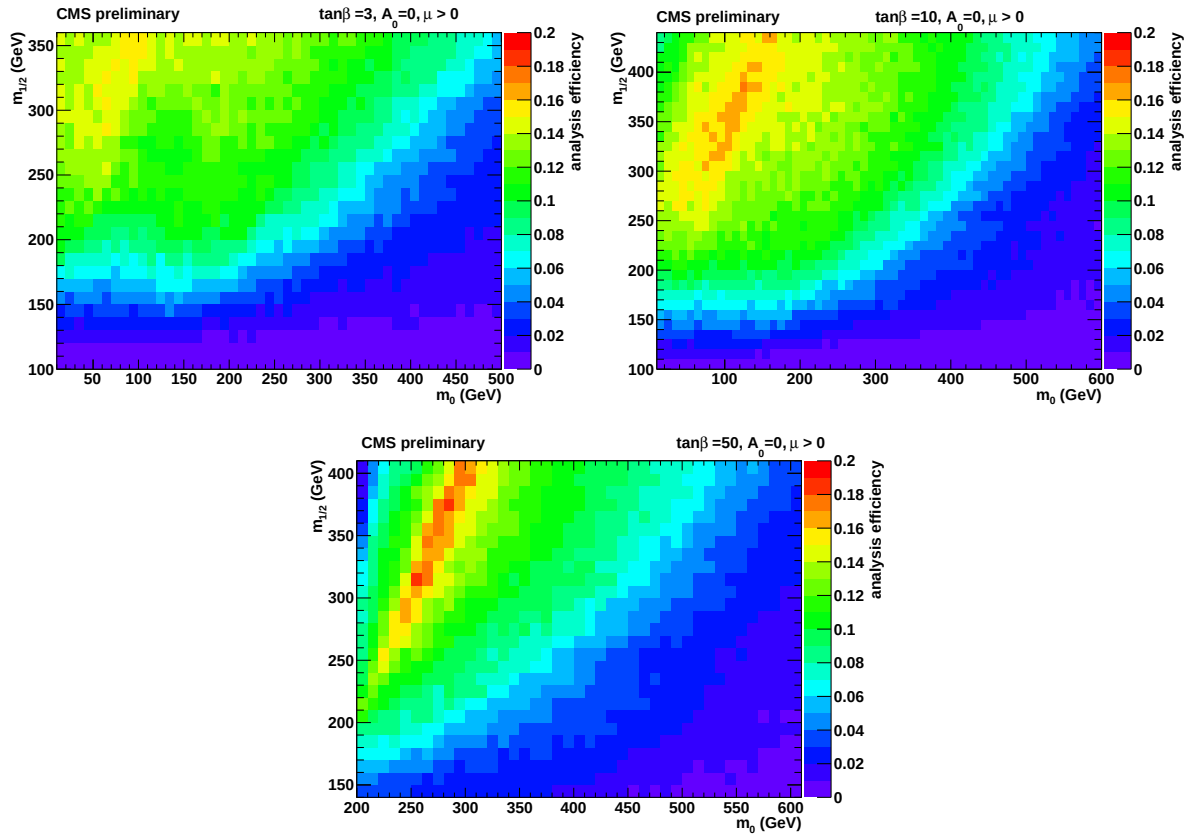

Figure 4: Analysis efficiency in the CMSSM $(m_0, m_{1/2})$ plane ($A_0 = 0$, $\mu > 0$) for $\tan\beta = 3$ (left), $\tan\beta = 10$ (right), and $\tan\beta = 50$ (bottom).

[1] Since the publication of Ref. [1], the uncertainty on the luminosity measurement reduced to 4% [11].

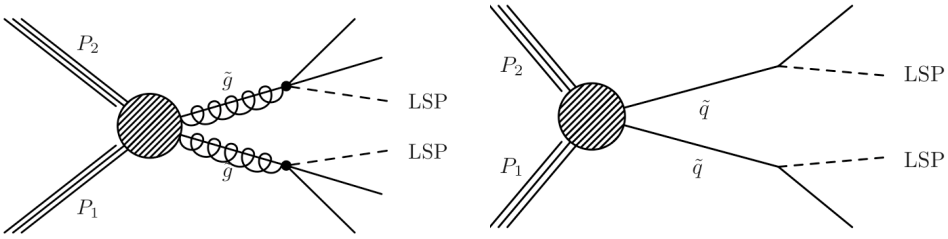

Figure 5: Diagram of simplified models. Top left: gluino pair production; top right: squark pair production. Both the gluon and the quark initiated production modes are used in the event generation.

4 Interpretation in the context of Simplified Model Spectra

The following description of the Simplified Model Spectra is based on Refs. [3–5] where they are described in detail.

In particular we consider:

- pair-produced gluinos where each gluino directly decays to two light quarks and the LSP;
- pair-produced squarks where each squark decays to one jet and the LSP.

Figure 5 shows the respective diagrams for the simplified topologies. Events samples produced with fast simulation [12] were generated for different combinations of squark (gluino) and LSP masses.

Figures 6 and 7 show the variation of the analysis efficiency (selection efficiency times acceptance) dependent on the gluino (squark) and LSP mass. The sample size is 10000 events for each point in the $(m_{\tilde{q}}, m_{\mathrm{LSP}})$ and $(m_{\tilde{g}}, m_{\mathrm{LSP}})$ parameter space. It can be seen that the efficiency of the analysis is much reduced in regions of parameter space where the squark (gluino) and LSP masses are similar, as in this case the production of hard jets is suppressed. The efficiency is highest for heavy squarks (gluinos) and LSP mass roughly half the squark (gluino) mass which leads to hard jets and sizeable missing transverse momentum.

In addition, Figures 6 and 7 show the experimental and theoretical uncertainties on the analysis efficiency, respectively. The experimental uncertainties include the same components as listed in Section 3.2, however, the uncertainty on the integrated luminosity of 11% is not included in the figure [2]. The only difference with respect to the treatment in Section 3.2 is that the uncertainty on the jet energy scale and resolution have been evaluated separately for every point in parameter space. This uncertainty is generally 2-3% where $m_{\tilde{g}}(m_{\tilde{q}}) \gg m_{\mathrm{LSP}}$. However, for points along the diagonal where $m_{\tilde{g}}(m_{\tilde{q}}) - m_{\mathrm{LSP}} < 200\,\mathrm{GeV}$ it can increase to $\sim$ 10-15%. As the production of high p_{T} jets is suppressed in this region of parameter space, threshold effects on the jet p_{T} requirements play a larger role.

The theoretical uncertainties on the analysis efficiency include variations of the parton distribution functions (PDFs). These have been evaluated following the prescription given in [13], us-

[2] While the uncertainty on the luminosity measurement has since reduced to 4% [11], the results presented here continue to use 11% for consistency with Ref. [1]

ing PDF sets provided by CTEQ6.6 [14], MSTW2008 [15] and NNPDF2.0 [16]. The uncertainties are propagated using the 68% envelope provided by the central values and the PDF+α_s errors of the three PDF sets. For most regions of $(m_{\tilde{g}}(m_{\tilde{q}}), m_{\mathrm{LSP}})$ parameter space these uncertainties are at the level of 5%. Only for large $m_{\tilde{g}}(m_{\tilde{q}})$ (> 700 GeV) and $m_{\tilde{g}}(m_{\tilde{q}}) - m_{\mathrm{LSP}} < 100\,\mathrm{GeV}$ they can reach up to 20%.

Furthermore, uncertainties due to initial state radiation (ISR) effects are taken into account (final state radiation effects were found to be negligible in comparison). As with the previously discussed uncertainties, ISR effects are relatively small and below 5% for the majority of parameter space. However, they become larger where $m_{\tilde{g}}(m_{\tilde{q}}) \sim m_{\mathrm{LSP}}$ and can become up to $\sim$30% for small $m_{\tilde{g}}(m_{\tilde{q}})$. In Figures 6 and 7 the theoretical uncertainties due to PDF variations and ISR effects were added in quadrature.

Figures 8 and 9 show the upper 95% C.L. limit on the cross section, with and without theoretical uncertainties included, for the T1 and T2 topologies, respectively. The same predictions as for the SM backgrounds in Section 2 are used. In the case of the simplified modes, only background contamination in the low H_{T} control region has been taken into account as these signatures do not produce isolated leptons or photons that could contaminate the muon and photon control samples. As a result of signal contamination in the background samples and parameter space dependent uncertainties on the signal efficiency, there is no direct correspondence between analysis efficiency and excluded cross section.

Furthermore, "reference cross sections" σ^{prod} for squark pair production (in the limit of decoupled gluinos) and gluino pair production (in the limit of decoupled squarks) through QCD interactions have been calculated at next to leading order precision using PROSPINO [17] and PDF CTEQ6L1 [18]. To give the reader an idea of the sensitivity of the current data to processes with such cross sections, contours where $(\sigma \times \mathrm{BR})_{95\%\mathrm{CL}} = \sigma^{\mathrm{prod}}$ and $(\sigma \times \mathrm{BR})_{95\%\mathrm{CL}} = 3 \times \sigma^{\mathrm{prod}}$ are overlaid on the cross section limits.

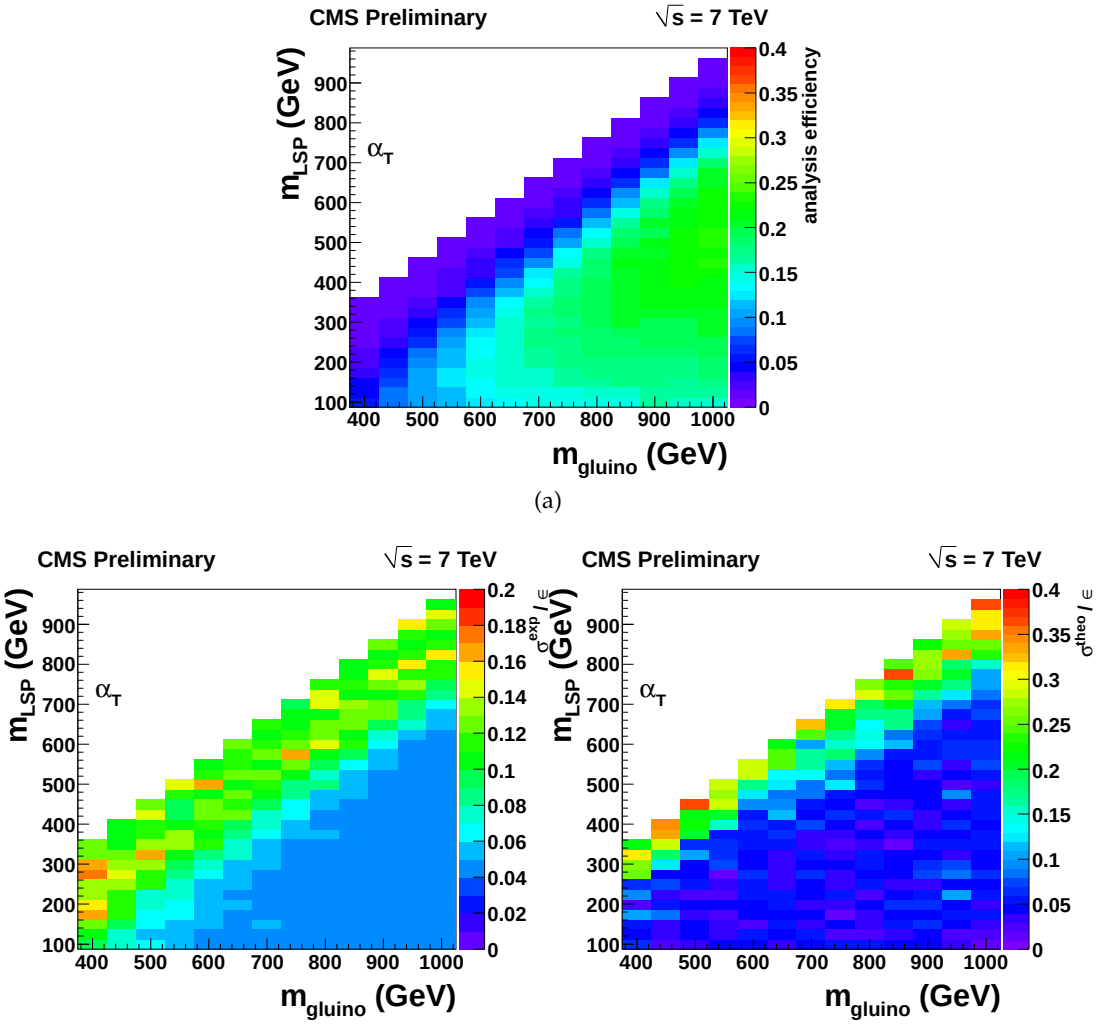

(a)

(b) (c)

Figure 6: (a) Analysis efficiency for gluino pair production a function of $m_{\tilde{g}}$ and m_{LSP}. (b) Experimental and (c) theoretical uncertainty on the analysis efficiency. Details on what contributions are considered in each case are given in the text.

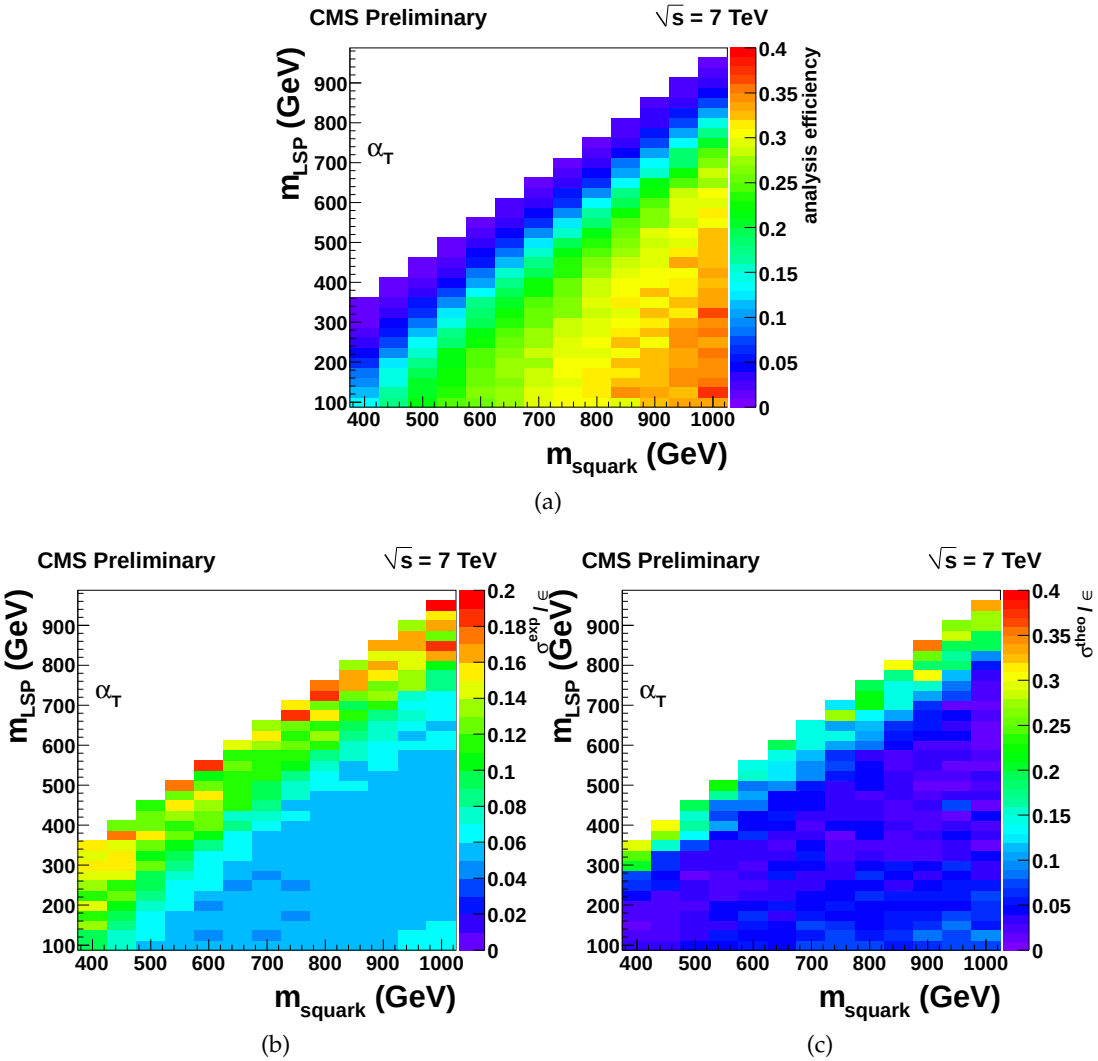

(a)

(b) (c)

Figure 7: (a) Analysis efficiency for squark pair production as a function of $m_{\tilde{q}}$ and m_{LSP}. (b) Experimental and (c) theoretical uncertainty on the analysis efficiency. Details on what contributions are considered in each case are given in the text.

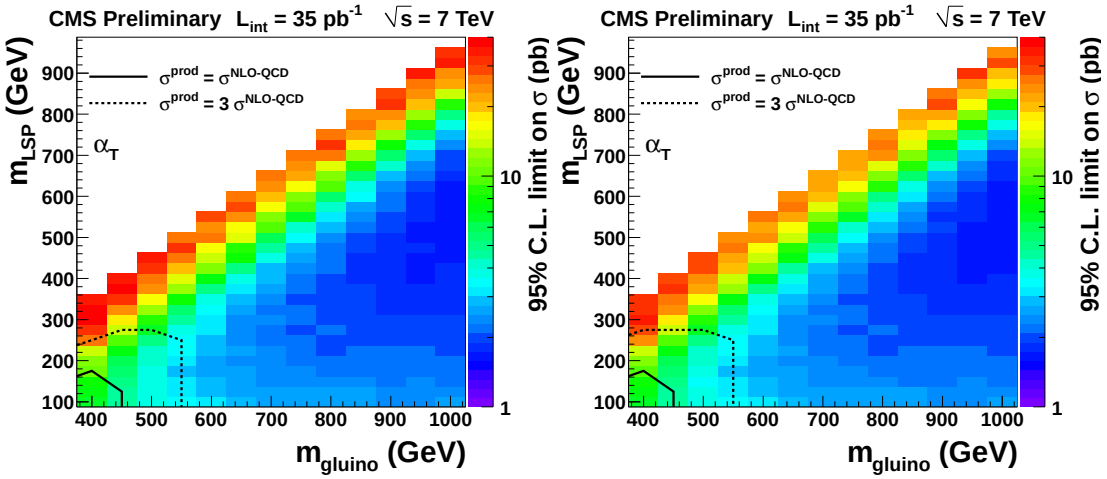

(a) (b)

Figure 8: Cross section for the gluino pair production topology excluded at the 95% CL. Overlaid are the excluded regions of parameter space using the reference cross sections σ^{prod}. Left: including theoretical uncertainties; Right: not including theoretical uncertainties.

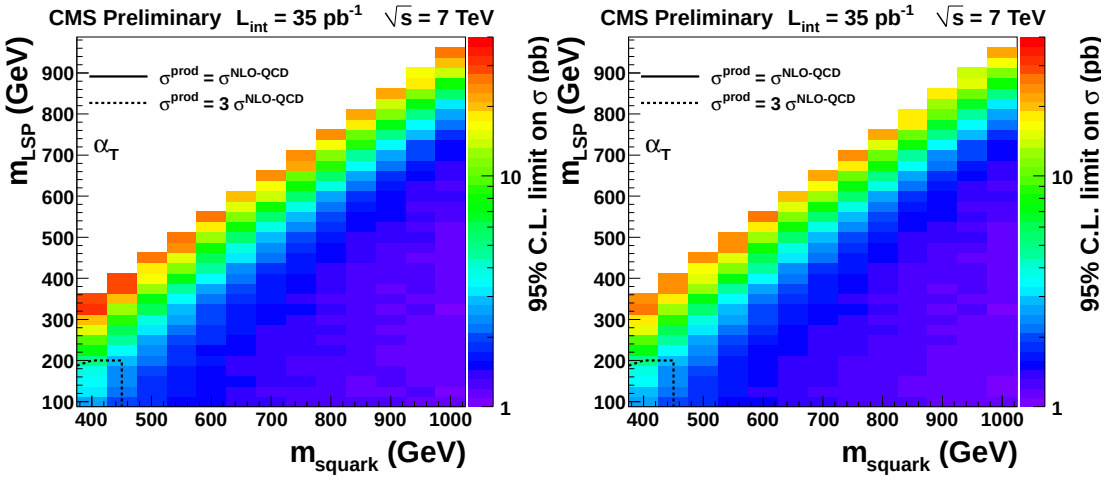

(a) (b)

Figure 9: Cross section for the squark pair production topology excluded at the 95% CL. Overlaid are the excluded regions of parameter space using the reference cross sections σ^{prod}. Left: including theoretical uncertainties; Right: not including theoretical uncertainties. (The contour with $(\sigma \times \text{BR})_{95\%\text{CL}} = \sigma^{\text{prod}}$ is not visible in the figure.)

5 Summary

We have presented additional material and interpretations of the analysis "*Search for Supersymmetry in pp Collisions at 7 TeV in Events with Jets and Missing Transverse Energy*" [1]. This material includes efficiency maps of the analysis in the $(m_0, m_{1/2})$ plane of the CMSSM as well as exclusion limits in the same plane for values of $\tan\beta = 10$ and 50. Furthermore, we have interpreted the search results in the more generic Simplified Model Spectra with squark and gluino pair production and set upper limits on the production cross section for these models depending on squark (gluino) and LSP mass. The efficiency maps and cross section limits presented here can be downloaded in electronic format from [19].

References

[1] CMS Collaboration Collaboration, "Search for Supersymmetry in pp Collisions at 7 TeV in Events with Jets and Missing Transverse Energy", *Phys. Lett.* **B698** (2011) 196, arXiv:1101.1628. doi:10.1016/j.physletb.2011.03.021.

[2] G. L. Kane, C. F. Kolda, L. Roszkowski et al., "Study of constrained minimal supersymmetry", *Phys. Rev.* **D49** (1994) 6173. doi:10.1103/PhysRevD.49.6173.

[3] LHC New Physics Working Group Collaboration, "Simplified Models for LHC New Physics Searches", *to be published* (June, 2010). http://www.lhcnewphysics.org.

[4] J. Alwall, P. Schuster, and N. Toro, "Simplified Models for a First Characterization of New Physics at the LHC", *Phys. Rev.* **D79** (2009) 075020, arXiv:0810.3921. doi:10.1103/PhysRevD.79.075020.

[5] J. Alwall, M.-P. Le, M. Lisanti et al., "Model-Independent Jets plus Missing Energy Searches", *Phys.Rev.* **D79** (2009) 015005, arXiv:0809.3264. doi:10.1103/PhysRevD.79.015005.

[6] M. Cacciari, G. P. Salam, and G. Soyez, "The anti-kt jet clustering algorithm", *JHEP* **0804:063** (2008). doi:10.1088/1126-6708/2008/04/063.

[7] CMS Collaboration, "Calorimeter Jet Quality Criteria for the First CMS Collision Data", *CMS Physics Analysis Summary* **JME-09-008** (2009).

[8] CMS Collaboration, "Electron reconstruction and identification at $\sqrt{s} = 7$ TeV", *CMS Physics Analysis Summary* **EGM-10-004** (2010).

[9] CMS Collaboration, "Performance of muon identification in pp collisions at $\sqrt{s} = 7$ TeV", *CMS Physics Analysis Summary* **MUO-10-002** (2010).

[10] CMS Collaboration, "Photon reconstruction and identification at $\sqrt{s} = 7$ TeV", *CMS Physics Analysis Summary* **EGM-10-005** (2010).

[11] CMS Collaboration, "Absolute luminosity normalization", *CMS Detector Performance Summary* **DP-2011-002** (2011).

[12] CMS Collaboration, "Comparison of the Fast Simulation of CMS with the first LHC data", *CMS Detector Performance Summary* **DP-2010-039** (2011).

[13] D. Bourilkov, R. C. Group, and M. R. Whalley, "LHAPDF: PDF use from the Tevatron to the LHC", arXiv:hep-ph/0605240.

[14] Nadolsky, Pavel M. et. al., "Implications of CTEQ global analysis for collider observables", *Phys. Rev.* **D78** (2008) 013004. doi:10.1103/PhysRevD.78.013004.

[15] A. D. Martin, W. J. Stirling, R. S. Thorne et al., "Parton distributions for the LHC", *Eur. Phys. J.* **C63** (2009) 189–285, arXiv:0901.0002. doi:10.1140/epjc/s10052-009-1072-5.

[16] R. D. Ball et al., "A first unbiased global NLO determination of parton distributions and their uncertainties", *Nucl. Phys.* **B838** (2010) 136–206, arXiv:1002.4407. doi:10.1016/j.nuclphysb.2010.05.008.

[17] W. Beenakker, R. Hopker, M. Spira et al., "Squark and gluino production at hadron colliders", *Nucl. Phys.* **B492** (1997) 51–103. doi:10.1016/S0550-3213(97)00084-9.

[18] J. Pumplin et al., "New generation of parton distributions with uncertainties from global QCD analysis", *JHEP* **07** (2002) 012, arXiv:hep-ph/0201195.

[19] https://twiki.cern.ch/twiki/bin/view/CMSPublic/PhysicsResultsSUS11001.